

Slag formation in silicon and ferrosilicon production using quartz, limestone and iron source

Sarina Bao and Eli Ringdalen

Cite this article as:

Sarina Bao and Eli Ringdalen, Slag formation in silicon and ferrosilicon production using quartz, limestone and iron source, *Int. J. Miner. Metall. Mater.*, 32(2025), No. 4, pp. 859-868. <https://doi.org/10.1007/s12613-024-3052-z>

View the article online at [SpringerLink](#) or [IJMMM Webpage](#).

Articles you may be interested in

Min Lin, Zhen-yu Pei, Yuan-yuan Liu, Zhang-jie Xia, Kang Xiong, Shao-min Lei, and En-wen Wang, [High-efficiency trace Na extraction from crystal quartz ore used for fused silica-A pretreatment technology](#), *Int. J. Miner. Metall. Mater.*, 24(2017), No. 10, pp. 1075-1086. <https://doi.org/10.1007/s12613-017-1498-y>

Yuri-Mikhailovich Grishin, Long Miao, Lev-Alekseevich Borisov, Nikolay-Mikhailovich Serykh, and Alexey-Yurievich Kulagin, [Applications of two electric arc plasma torches for the beneficiation of natural quartz](#), *Int. J. Miner. Metall. Mater.*, 26(2019), No. 3, pp. 267-273. <https://doi.org/10.1007/s12613-019-1734-8>

Yan-ping Niu, Chuan-yao Sun, Wan-zhong Yin, Xing-rong Zhang, Hong-feng Xu, and Xu Zhang, [Selective flotation separation of andalusite and quartz and its mechanism](#), *Int. J. Miner. Metall. Mater.*, 26(2019), No. 9, pp. 1059-1068. <https://doi.org/10.1007/s12613-019-1842-5>

Xu-zhong Gong, Jun-qiang Zhang, Zhi Wang, Dong Wang, Jun-hao Liu, Xiao-dong Jing, Guo-yu Qian, and Chuan Wang, [Development of calcium coke for \$\text{CaC}_2\$ production using calcium carbide slag and coking coal](#), *Int. J. Miner. Metall. Mater.*, 28(2021), No. 1, pp. 76-87. <https://doi.org/10.1007/s12613-020-2049-5>

Yong-sheng Sun, Yue-xin Han, Yan-feng Li, and Yan-jun Li, [Formation and characterization of metallic iron grains in coal-based reduction of oolitic iron ore](#), *Int. J. Miner. Metall. Mater.*, 24(2017), No. 2, pp. 123-129. <https://doi.org/10.1007/s12613-017-1386-5>

Lei Zhang, Hui-xin Li, Feng-xian Shi, Jian-wei Yang, Li-hua Hu, and Min-xu Lu, [Environmental boundary and formation mechanism of different types of \$\text{H}_2\text{S}\$ corrosion products on pipeline steel](#), *Int. J. Miner. Metall. Mater.*, 24(2017), No. 4, pp. 401-409. <https://doi.org/10.1007/s12613-017-1420-7>



IJMMM WeChat



QQ author group

Slag formation in silicon and ferrosilicon production using quartz, limestone and iron source

Sarina Bao[✉] and Eli Ringdalen

SINTEF Industry, SINTEF, Alfred Getz Vei 2B, Trondheim 7034, Norway

(Received: 27 August 2024; revised: 20 November 2024; accepted: 21 November 2024)

Abstract: The production processes for Si and FeSi have traditionally been considered slag-free. However, recent excavations have revealed significant accumulation of CaO–SiO₂–Al₂O₃ slag within the furnaces. This accumulation can obstruct the flow of materials and gases, resulting in lower metal yield and higher energy consumption. The main objective of the current work is to enhance our understanding of slag formation during Si and FeSi production. We investigate slag formation through the dissolution of limestone and iron oxide in quartz and condensate, focusing on the reactions between these materials at a gram scale. Our findings indicate that most slag reaches equilibrium relatively quickly at temperatures starting from 1673 K. Notably, slag formation starts at lower temperature when the iron source is present (1573 K) compared to when only CaO is involved (1673 K). The minor elements tend to accumulate at quartz grain boundaries prior to slag formation. Furthermore, the slag produced from condensate contains less SiO₂ than that generated from quartz with limestone. The type of quartz source and SiO₂ phase appears to have little influence on slag formation. Good wettability is a significant factor in reaction between quartz and slag. FactSage calculations indicates that the viscosity of the slag ranges from 0.02 to 14.4 Pa·s under furnace conditions, comparable to the viscosity of honey or motor oil at room temperature.

Keywords: slag formation; silicon and ferrosilicon production; quartz; limestone; iron source; condensate; cristobalite

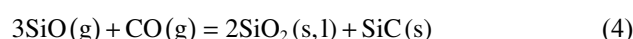
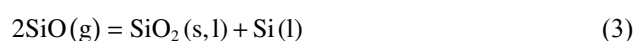
1. Introduction

Silicon (Si) and silicon alloys are produced in submerged arc furnaces (SAF), which operate at extremely high temperatures to facilitate reduction reactions. The primary raw materials are quartz (SiO₂) and carbon-based reductants, such as coal or coke, which drive the reduction process that yields silicon metal. In ferrosilicon (FeSi) production, an additional iron source is added to the furnace charge [1]. The primary silicon production takes place in a high-temperature cavity surrounding the electrode tip, where intense energy input promotes reduction reactions [2].

Around the furnace cavity, a solid crust forms, primarily composed of silicon carbide (SiC) [3], which insulates the cavity. In the core reduction zone, SiO gas [4–5] is generated and rises within the furnace. As it ascends, the SiO gas reacts with carbon to form additional SiC or condenses to create a deposit of Si, SiO₂, and SiC on the surrounding materials. This condensate layer [6] can restrict gas flow and reduce permeability, impacting overall efficiency by obstructing the upward movement of reaction gases. Managing this layer is crucial for ensuring optimal gas flow, maintaining energy efficiency, and achieving high purity in the silicon or ferrosilicon produced.

The reduction of silica to Si occurs through the overall reaction (1). In industrial furnaces, this process unfolds through

multiple steps as outlined by Schei *et al.* [7]. Raw materials, including quartz, carbon materials (such as coke, coal, charcoal, and wood chips), and iron oxide or scrap iron (for FeSi production) are fed from the top of the furnace. In the upper furnace zone, descending raw materials encounter ascending SiO and CO gas. Here carbon reacts with SiO to form SiC by reaction (2) [8]. The ascending gases also condense in the cooler temperature zone [9] following reactions (3)–(4). In furnace's lower section, at temperatures above 2123 K, Si production occurs via reaction (5). SiO gas required for this reaction and for SiC production in the upper furnace is generated from SiO₂ through reactions (6)–(7). The stability and predominance of these reactions are highly influenced by the partial pressures of SiO and CO gases, which are critical to the furnace's efficiency and output quality [10].

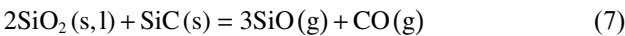


The reactions (2)–(4) are exothermic reactions, and reactions (5)–(7) are the endothermic reactions in the lower furnace and around the crater.



✉ Corresponding author: Sarina Bao E-mail: sarina.bao@sintef.no

© The Author(s) 2025



Traditionally Si and FeSi processes are considered slag-free with minimal slag formation expected. However, excav-

ations of industrial furnaces, as illustrated in Fig. 1, reveal that substantial slag can accumulate inside the furnace [3]. Even though zones within FeSi furnaces differ significantly, deposited slag along with pre-melted raw materials are often found in inactive areas. This slag typically consists of SiO_2 -

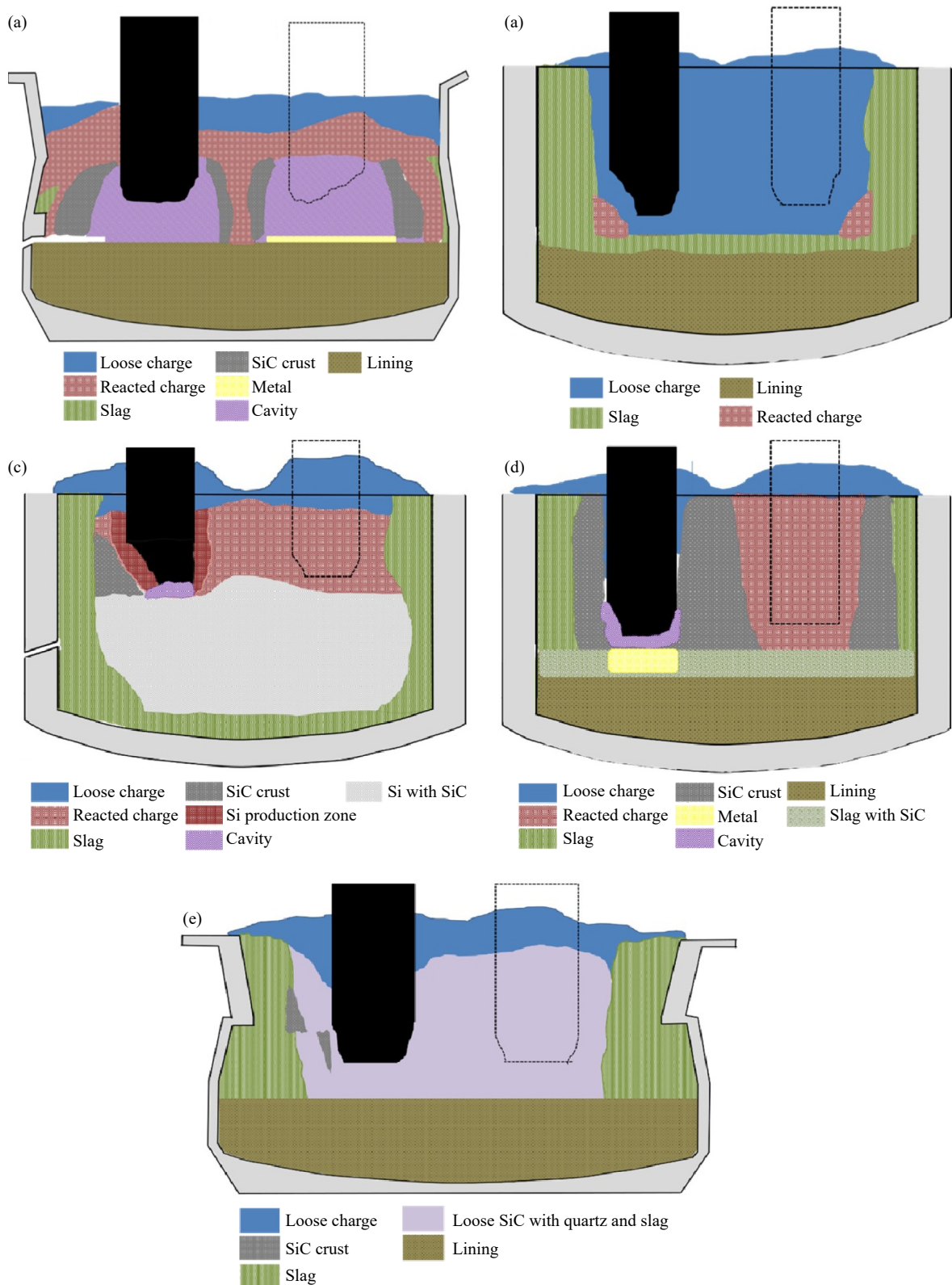


Fig. 1. Overview of zones in FeSi and Si furnaces: (a) 75% FeSi in Finnjord; (b) 50% FeSi in Elkem Bjølvfosen; (c) Wacker furnace No. 1, Si; (d) Si in Elkem Thamshavn; (e) Wacker furnace No. 4, Si. The slag is shown by light green. Reprinted with permission from Ref. [3].

CaO–Al₂O₃ in various proportions. Observations show that a layer of liquid slag and SiC particles may encase silicon within the tap hole channel [11]. Calcium (Ca) and aluminium (Al), introduced either as trace elements in the raw materials or as separate fluxes, are largely tapped alongside the liquid metal. This suggests that the buildup of significant amounts of Ca- and Al- containing slags may take place gradually over time.

In Si/FeSi production, both solid and molten SiO₂ from quartz are typically present throughout the furnaces. Additionally, molten SiO₂ formed through the “condensation” of SiO gas, often exists within the furnace, usually mixed closely with Si and/or SiC. These forms of SiO₂ are not regarded as slag. For material to be classified as slag in this context, it must contain over 10wt% of other oxides, in addition to SiO₂ [12]. Slag forms when other compounds react with, coalesce with, or dissolve in quartz, and its composition changes as either quartz or other oxides are introduced.

The composition of the formed slag may either be determined by the equilibrium among all compounds under furnace conditions or by kinetic factors. In the latter case, equilibrium may not be achieved between one or more compounds within the available time and temperature range in the furnace. There is limited information on slag formation in Si and FeSi processes. Due to the high viscosity of quartz at low temperature [13], it is likely that equilibrium between quartz and the slag phase is not reached. However, when slag mixes with additional components, both its liquidus temperature and viscosity decrease rapidly. Trace elements in the gangue minerals within quartz, such as K₂O will also help lower slag viscosity and liquidus temperature, potentially enhancing slag formation.

To better understand slag formation in Si and FeSi furnaces and the effect of different raw material properties, more knowledge is needed on reaction mechanisms, equilibrium

conditions, and kinetics. This study investigates slag formation from reactions between SiO₂ and sources of limestone or iron.

Experimental analysis focused on several key phenomena: slag formation at the grain boundaries and interfaces, composition gradient extending towards pure quartz, slag composition within quartz cracks and at particle boundaries, effect of slag formation on elements dissolution, role of minor element at the grain boundaries in dissolution processes, wettability of quartz by slag, and slag viscosity.

2. Experimental

In Si and FeSi furnaces, quartz, limestone, and iron source are the primary raw materials. The current work handles two industrial quartz sources, a condensate, two cristobalites derived from two quartz sources, limestone and lime (calcinated limestone to remove CO₂ influence), as well as iron source and pure FeO (to isolate the effects of the impurities in iron source). This selection enables a detailed investigation of slag formation under controlled conditions. The percentages of the main components are presented in Table 1. Since K₂O affects liquidus temperatures, viscosity, and wettability, its content is included alongside the primary elements. The percentages of the normalized main components were calculated from the chemical analysis, with the assumption that for quartz, difference to 100% is SiO₂, for iron sources it is Fe₂O₃, and for limestone, it is CO₂. No accumulation of any components was observed around the cracks in the raw quartz. The investigated quartz samples, Qz47 and Qz54 were both sourced from industrial operations. Additionally, Qz54, along with limestone and iron source, was specifically supplied for this investigation by the ferrosilicon producer Finnfjord AS, Norway.

Table 1. Normalized chemical composition of raw materials

Material	SiO ₂	Fe ₂ O ₃	CaO	Al ₂ O ₃	CO ₂	K ₂ O	Total
Quartz Qz47	99.706	0.007	0.240	0.026		0.013	100
Quartz Qz54	99.000	0.025	0.003	0.542		0.112	100
Limestone	0.986	0.267	55.468	0.113	43.142	0.024	100
Iron source	4.047	94.320	0.672	0.962		0	100

Condensate was collected from the charge surface of a FeSi furnace in Finnfjord AS. It was viscous at sampling time while the area around the sample was hard. The piece used in current work is a condensate consisting of SiO₂ and Si (made by reactions (3) and (4)) surrounded by several layers of Si droplet and a combination of SiO₂ and SiC [14]. The primary composition of the condensate consists of SiO₂ and Si in mole ratio of 1:0.7 with K₂O and MgO accumulating at the grain boundaries. Notably, the condensate is free of cracks, unlike the quartz.

Cristobalite for the investigations was produced by heating quartz at a rate of 50 K/min to 1873 K (1600°C) and holding it at that temperature for 2 h. CO₂ in the limestone is

expected to be released at temperatures above 1473 K (1200°C), meaning that in industrial furnaces, the limestone will have already reacted to form CaO before reaching the temperatures at which the slag formation begins. Prior to the experiments, limestone was calcined by heating 6 K/min to 1273 K (1000°C) and holding it for 1 h in a muffle furnace. The calcined product, lime was removed at around 373 K (100°C) and transferred to a drying furnace set at 378 K (105°C) to prevent moisture absorption.

All quartz, limestone, and iron source were drilled and cut into cylinders measuring $\phi 3$ mm \times 3 mm before being placed onto a substrate. Both quartz samples were drilled and cut into $\phi 10$ mm \times 3 mm cylinders for used as substrate. The con-

densates were broken into small pieces for further analysis.

Slag formation was investigated using sessile drop furnace, as introduced by the same author [15]. Samples measuring approximately 3 mm were placed on a 10-mm diameter SiC or graphite substrate and heated under a 0.1 L/min flow of 6N grade Ar (99.9999%) atmosphere. The samples were heated to 1173 K (900°C) in about 3 min, followed by a constant rate increase of 50 K/min to either 1373 K (1100°C) or 1573 K (1300°C), and then to the designated temperature at a rate of 5.5 K/min. High-resolution video and images were employed to assess the softening, melting, wetting, and coalescence behavior. Samples after the test were cut and examined using a scanning electron microscope (SEM) equipped with wavelength dispersive spectroscopy (WDS) to investigate the dissolution mechanism and diffusion of elements. The thermocouple was periodically calibrated using iron (Fe), with melting temperature of 1811 K (1538°C) under the same experimental conditions, typically requiring less than a 10 K adjustment for most tests. The values discussed in the current paper are without correction. FactSage Version 8.2, along with the FToxid database, was used to calculate the phase diagram and viscosity of the slag system.

3. Results and discussion

3.1. Slag formation by quartz (SiO_2) reacting with limestone/lime

Coalescence of quartz and limestone occurs at temperatures starting from 1623 K (1350°C). Fe and Al oxides were observed in cracks and grain boundaries of quartz, while CaO was present at the grain boundaries of limestone before coalescence. As the temperature increases, the formation of SiO_2 -CaO becomes more pronounced. The quartz source does not appear to significantly influence slag formation. For instance, when using the purer quartz Qz47, the resulting slag formation, as shown in Fig. 2, is similar to that for quartz Qz54. Typically, the amounts of SiO_2 and CaO in slag account for over 90wt% of the oxide species, which include SiO_2 , CaO, NaO, MnO, MgO, FeO, Al_2O_3 , TiO_2 , and K_2O . Consequently, the composition of SiO_2 and CaO was normalized to 100wt%. The same analytical method was applied to the SiO_2 -FeO and SiO_2 -FeO-CaO slag systems. In the binary slag CaO- SiO_2 , the SiO_2 content ranges from 49wt% to 67wt% until the SiO_2 /CaO mole ratio reaches approximately 1.5 to 1.6 at temperatures between 1823 K (1550°C) and 1873 K (1600°C), as illustrated in Fig. 3.

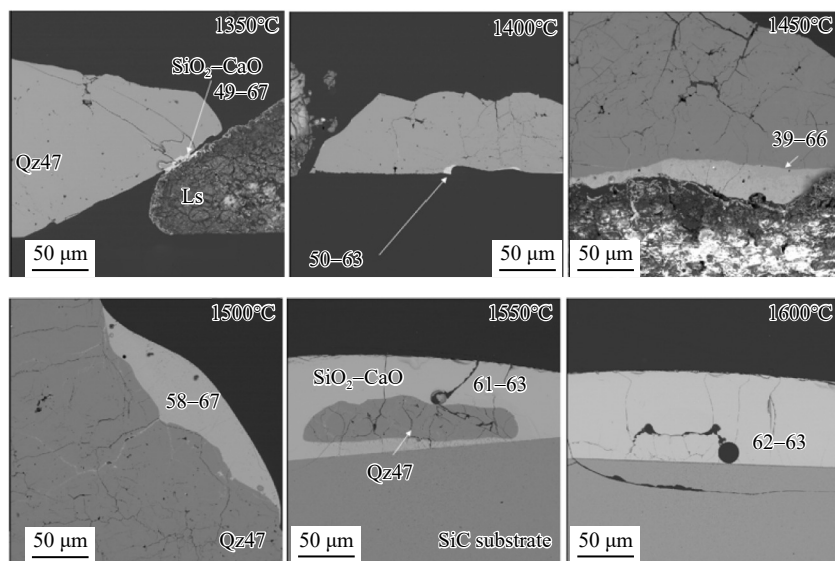


Fig. 2. Microscopic analysis of slag formation by quartz Qz47 reacting with limestone at different temperature. Ls is limestone. SEM backscatter images with analysis from WDS. Values in the figure are SiO_2 content in slag (wt%).

Lime reacts with quartz or cristobalite derived from quartz to produce CaO- SiO_2 slag. Notably, all slags are found with-

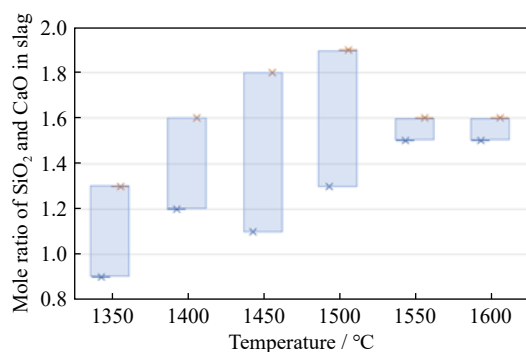


Fig. 3. SiO_2 /CaO mole ratio in slag outside quartz Qz47.

in the cristobalite cracks, rather than outside them. This suggests good wetting between slag and cristobalite; however, no wetting behavior can be observed otherwise. It is possible that the slag formed due to diffusion of CaO in a semi-liquid slag within the cracks, potentially influenced by contaminants and other minerals along grain boundaries or crack boundaries. The theoretical melting temperature of lime is 2845 K (2572°C). The SiO_2 -CaO slag exhibits excellent wetting properties with quartz. As illustrated in Fig. 4, the wetting angle decreases rapidly from 33° to 0° as the temperature rises from 1723 K (1450°C) to 1873 K (1600°C).

According to the binary phase diagram of SiO_2 -CaO in Fig. 5, the slag has an eutectic point at 62.9wt% SiO_2 at 1710 K (1437°C). During heating, CaO from limestone/lime and

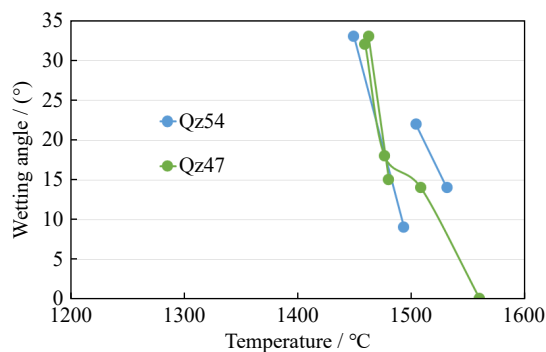


Fig. 4. Wetting of CaO–SiO₂ slag with quartz. Two parallel tests for both quartz sources, and four wetting angles were successfully measured for one parallel for Qz47, while two for the rest parallels.

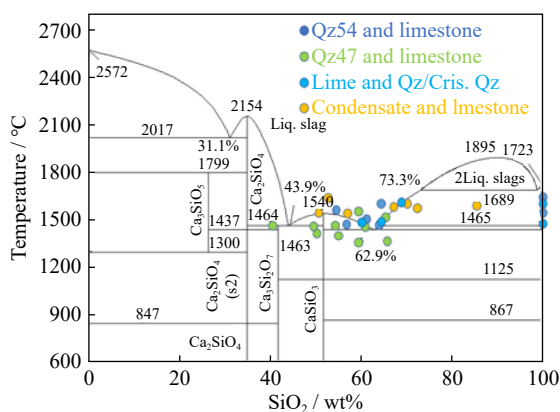


Fig. 5. SiO₂–CaO phase diagram calculated by Factsage ver. 8.2. The current SiO₂–CaO slags are marked. Liq.—Liquid; Qz—Quartz; Cris. Qz—Cristobalite derived from quartz.

SiO₂ from quartz/condensate/cristobalite generated from quartz form a liquid slag, which solidify upon cooling. As the liquid slag approaches equilibrium, it precipitates SiO₂ and Ca₂SiO₄ phases, following the liquidus–solidus line in phase diagram. The compositions of the slags investigated in this work represent liquid compositions at the investigated temperature due to rapid cooling and are situated at or near the liquidus lines. Consequently, most of the SiO₂–CaO slag formed in current work is believed to have reached the equilibrium from 1673 K (1400°C). The relatively small deviation in composition from the solidus–liquidus line is thought to result from uncertainties in the WDS analysis. Only the slag composition from outside the quartz is considered.

The composition of the slag has been measured at various locations within the samples. Although Figs. 6 and 7 suggest that the SiO₂ content at different locations does not appear to vary with temperature, the slag at the quartz interface and within quartz cracks would still be in equilibrium with the quartz, considering the steep slope of liquidus–solidus line in Fig. 5. The average SiO₂ content in CaO–SiO₂ slag located outside the quartz is approximately 60wt%. The width of slag within cracks ranges of several tens of micrometres along the quartz grain boundaries. Additionally, the content of the minor elements K₂O and FeO differ between the cracks in the quartz and the slag, with K₂O being more abundant along the

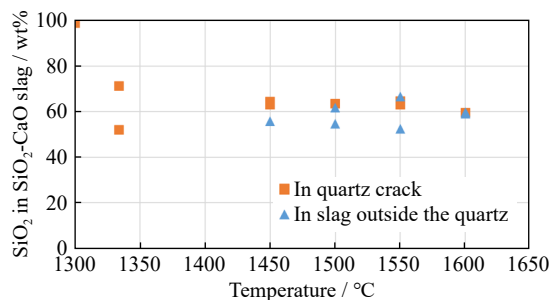


Fig. 6. SiO₂ content change in SiO₂–CaO slag by location and temperature for quartz Qz54 and limestone heated on SiC.

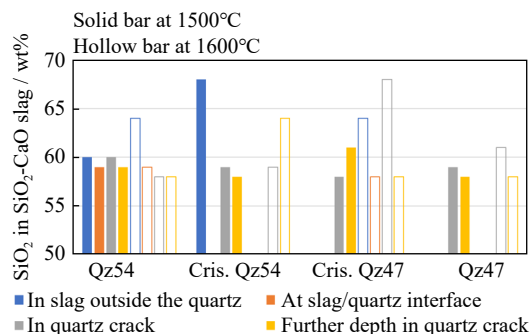


Fig. 7. SiO₂ content change in SiO₂–CaO slag by location and temperature for lime heated on quartz. Cris. Qz47 and Cris. Qz54 represent the cristobalite made from quartz Qz47 and Qz54, respectively.

quartz grain boundaries prior to slag formation. The concentrations of both FeO and K₂O in slag outside the quartz are less than 1wt%.

3.2. Slag formation by condensate reacting with limestone

SiO₂–CaO slag begins to form from 1773 K (1500°C) when the condensate reacts with limestone. As shown in Fig. 8, the SiO₂ content in the slag decreases with increasing temperature until it stabilizes at approximately 50wt%. The key difference between the reactions of quartz and limestone is that the slag formed from the condensate and limestone contains about 10wt% less SiO₂. Still the reaction between the condensate and limestone can be reached equilibrium, considering the steep slope of the liquidus–solidus line in Fig. 5.

3.3. Slag formation by quartz (SiO₂) reacting with iron source

The iron source exhibits excellent wetting properties with quartz Qz54 right after it completely melts at approximately 1573 K (1300°C). Subsequently, SiO₂–FeO slag starts to form (see Fig. 9). As the temperature increases, Fe droplet appear within slag, and the number of gas bubbles increases at 1973 K (1700°C), which are presumed to be trapped within the viscous slag. To minimize the influence of reaction with carbon substrate and from impurities, pure FeO powder was heated on a cristobalite derived from quartz Qz47. Multiple Fe droplets formed, and the FeO–SiO₂ slag sank into the cracks of the cristobalite. The composition of slag produced

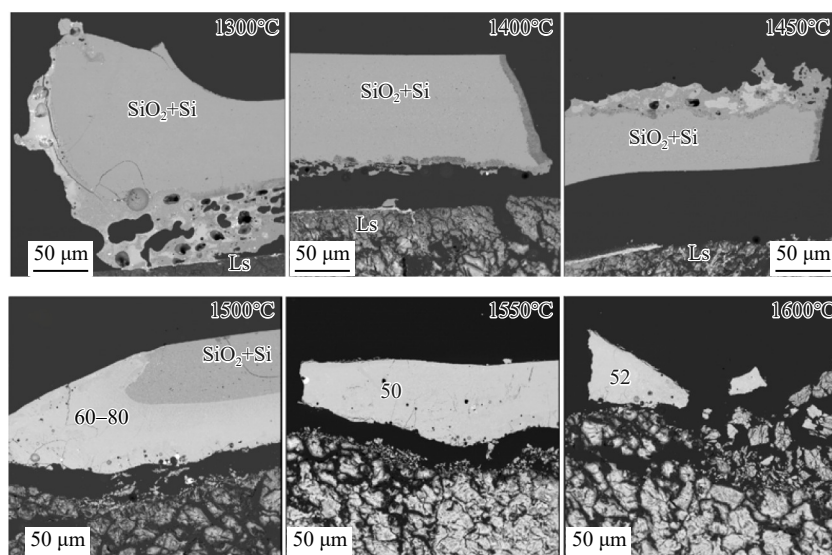


Fig. 8. Microscopic analysis of slag formation by condensate reacting with limestone at different temperature. Ls is limestone. SEM backscatter images with analysis from WDS. Values in the figure are SiO_2 content in slag (wt%).

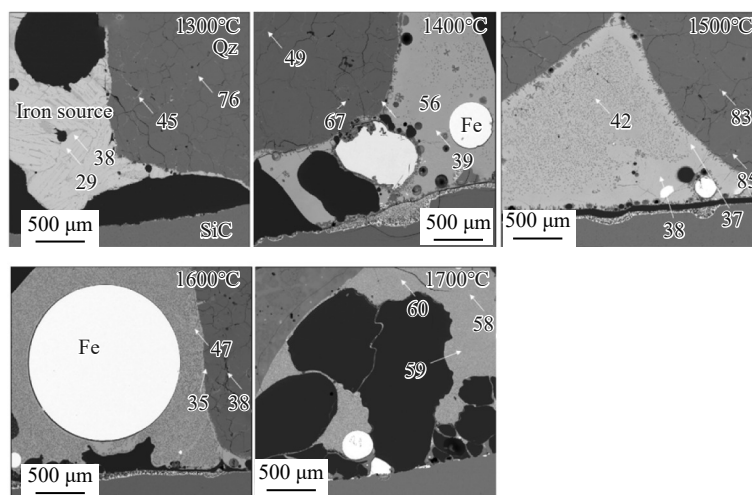


Fig. 9. Microscopic analysis of slag formation by iron source reacting with quartz Qz54 at different temperature. SEM backscatter images with analysis from WDS. Values in the figure are SiO_2 content in slag (wt%).

from pure FeO powder at the same temperature of 1873 K (1600°C) is quite similar to that obtained from the industrial iron source.

Fig. 10 summarizes the wettability of FeO– SiO_2 slag formed from iron source in reaction with various SiO_2 materials. The SiO_2 –FeO slag produced in this investigation demonstrates excellent wetting characteristics with both quartz and cristobalite made from quartz. The wetting angle ranging from 14° to 47°. Notably, the wettability remains relatively constant up to 1873 K (1600°C). In comparison to Fig. 4, CaO– SiO_2 slag shows better wetting with quartz than FeO– SiO_2 slag.

Fig. 11 indicates that the type of quartz source or cristobalite does not significantly influence the SiO_2 distribution in SiO_2 –FeO slag. Fe droplets form in liquid slag at 1773 K (1500°C) and 1873 K (1600°C), no matter the silica source. While the increased porosity of cristobalite appears to facilitate the rapid immersion of slag, the iron droplets do not penetrate the cracks, suggesting that Fe droplets do not wet cris-

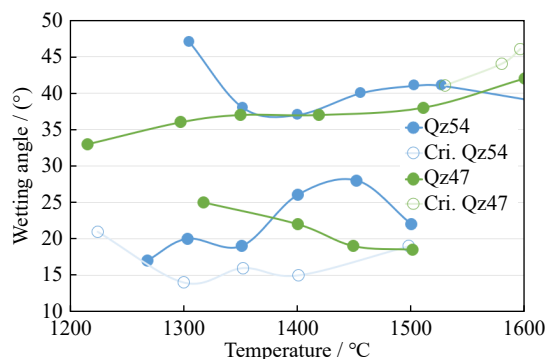


Fig. 10. Wetting of FeO– SiO_2 slag towards SiO_2 substrate made from quartz (Qz54 and Qz47) and cristobalites made from quartzs (Cri. Qz47 and Cri. Qz54).

tobalite or quartz as effectively as the slag does.

As illustrated in the binary phase diagram in Fig. 12, SiO_2 –FeO slag has eutectic points of 22wt% and 36.7wt% SiO_2 , occurring at 1461 K (1188°C). During solidification, the liquid slag precipitates SiO_2 and the composition of the

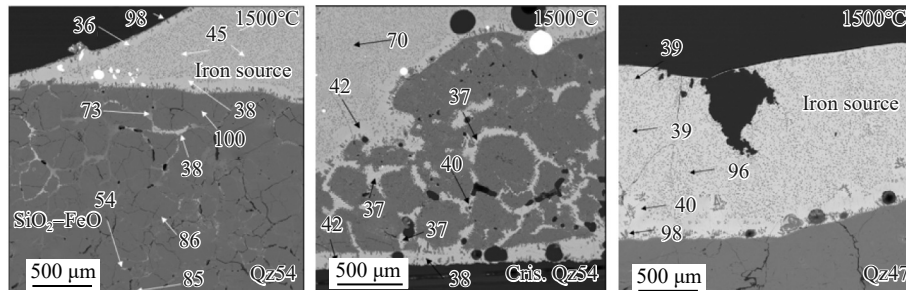


Fig. 11. Microscopic analysis of slag formation by iron source reacting with quartz Qz54 (left), cristobalite made from Qz54 (middle), and quartz Qz47 (right). SEM backscatter images with analysis from WDS. Values in the figure are SiO_2 content in slag (wt%).

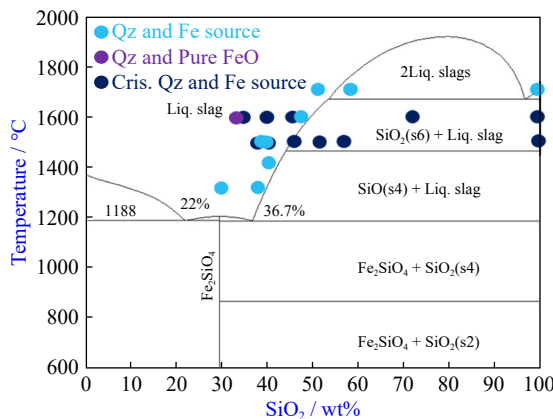


Fig. 12. SiO_2 -FeO phase diagram calculated by Factsage ver. 8.2. The current SiO_2 -FeO slags are marked.

liquid phases follows the liquidus–solidus line in the phase diagram when the liquid slag is in the equilibrium. The composition from the current investigations represents liquid composition at the investigated temperature due to fast cooling, with most samples being in equilibrium as shown in Fig. 12. However, the slag composition may deviate from the liquidus–solidus line due to uncertainties in analysis by WDS

analysis. Similar to SiO_2 -CaO slag, the SiO_2 amount in SiO_2 -FeO slag does not appear to change significantly with temperature or location, whether in slag outside quartz, at quartz-slag interface, or within cracks in the slag. The SiO_2 -FeO slag located outside the quartz contains approximately 40wt% SiO_2 . Moreover, quartz type and cristobalite does not seem to influence the SiO_2 distribution in the slag.

3.4. Slag formation by limestone reacting with iron source

As shown in Fig. 13, the coalescence of limestone and iron source starts from 1523 K (1250°C). Before this reaction commences, CaO is elevated in certain areas, appearing as white spots in the limestone at 1753 K (1300°C). The iron source exhibits excellent wetting with solid limestone, sometimes even lifting it. In most cases, the reaction product, SiO_2 -FeO-CaO ternary slag remains solid up to 1873 K (1600°C), with exception is the SiO_2 -FeO slag at 1873 K (1600°C).

The equilibrium composition and liquidus–solidus lines of the SiO_2 -CaO-FeO ternary slag are presented in Fig. 14. SiO_2 -CaO-FeO slags formed during the current investigations are plotted on the diagram, indicating the temperatures

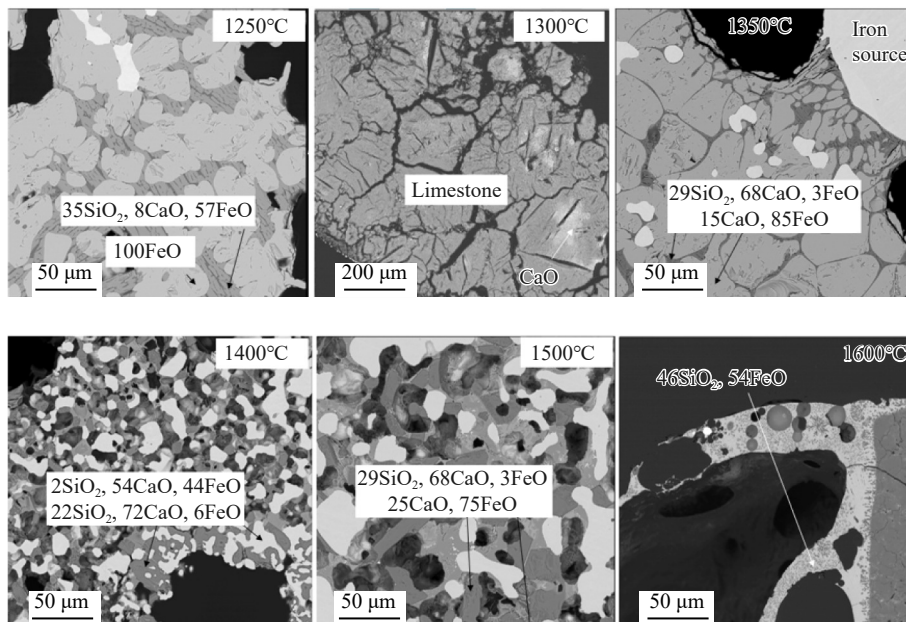


Fig. 13. Microscopic analysis of slag formation by iron source reacting with limestone. SEM backscatter images with analysis from WDS.

at which the tests concluded. During solidification, the liquid slag precipitates SiO_2 , CaO , or FeO , with phases adhering to the liquidus–solidus line in the phase diagram. Most of the SiO_2 – CaO – FeO slags formed in current work are situated below the liquidus and above the solidus at the test temperat-

ures, indicating they are mixtures of liquid and solid phases. Consequently, the slag must form by diffusion within the liquid phase. In contrast, the SiO_2 – FeO slag, marked in green in Fig. 14, remains liquid at its final test temperature, which facilitates the slag formation process.

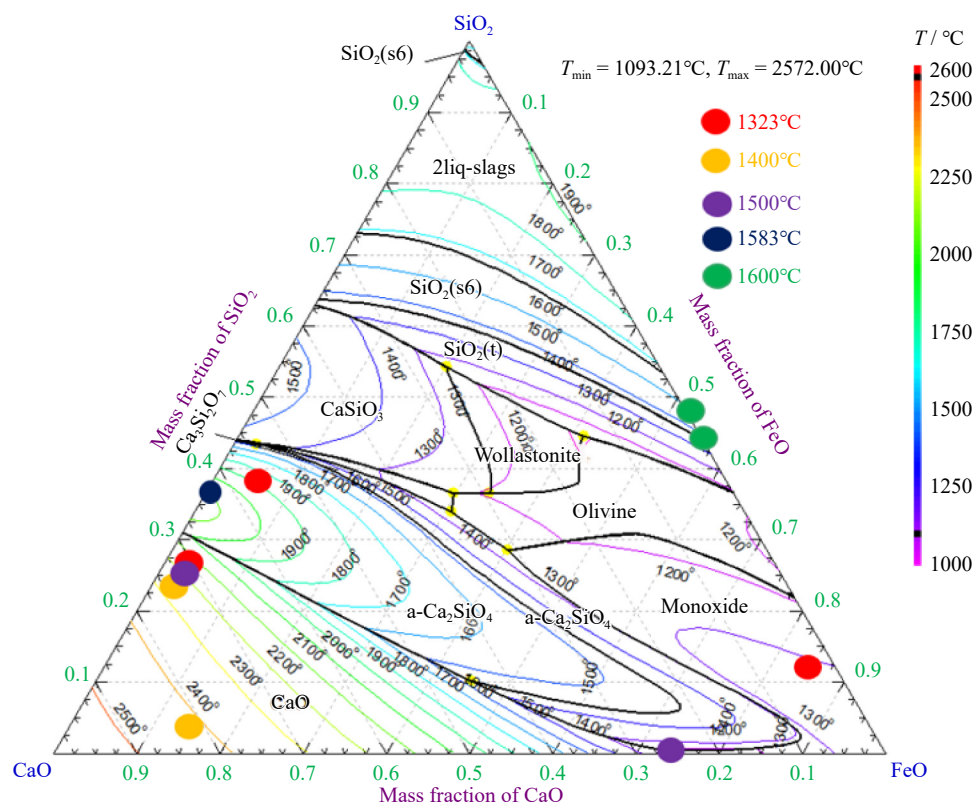


Fig. 14. SiO_2 – CaO – FeO phase diagram calculated by Factsage ver. 8.2. The ternary slag composition in the current work at each end test temperate is marked.

The SiO_2 content in solid slag was less than 34wt% in the SiO_2 – CaO – FeO slag, while it reached 48wt% in the FeO – SiO_2 liquid slag at 1873 K (1600°C). The iron source begins to melt at 1583 K (1310°C), as illustrated in Fig. 15, and FeO reacts with other phases until saturation, as depicted in Fig. 13. Although most of the slags formed are mixtures of liquid and solid phases at the selected temperature, dissolution is expected to be much slower than the other binary slags investigated in the current work, which were solely liquid.

3.5. Coalescence of quartz, limestone and iron source

Investigations into the softening and melting properties of the raw materials used in the current investigations reveal, as seen in Fig. 15, that quartz begins to soften at 2033 K (1760°C), limestone softens at 1963 K (1690°C), and completely melts at 2043 K (1770°C). In contrast, the iron source has a relatively low melting temperature, becoming fully molten at 1583 K (1310°C). The time interval between the onset of soften and total melting can be considered neglected for the iron source.

Coalescence, defined here as joining or merging of raw materials, occurs prior to the softening of these materials. It is reasonable to conclude that even though coalescence starts before the melting of the iron source, it likely completes

around or after the melting of the iron source when it reacts with quartz or limestone. Additionally, the coalescence of condensate reacting with limestone does not appear to vary from that of quartz reacting with limestone.

3.6. Viscosity

The viscosity of slag was calculated using FactSage ver 8.2 taking into account the contents of SiO_2 , CaO , FeO , Al_2O_3 , MgO , MnO , and TiO_2 at selected temperatures. The calculated viscosities pertain only to the liquid phase present

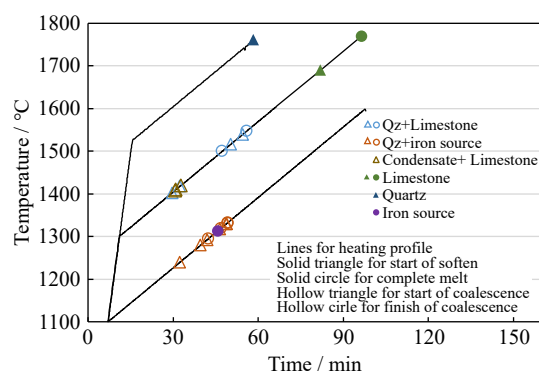


Fig. 15. Softening, melting, and coalescence of quartz, condensate, limestone, and iron source.

at the actual temperature, and do not account for the effect of solid equilibrium phases. In this study, the viscosity of the $\text{SiO}_2\text{--CaO}$ slag ranges from 0.4 to 14.4 Pa·s while the viscosity of the formed $\text{SiO}_2\text{--FeO}$ slags ranges from 0.02 to 7.13 Pa·s. The $\text{SiO}_2\text{--CaO--FeO}$ ternary slag remains solid at the selected temperatures up to 1873 K (1600°C). So no viscosity was calculated for that phase.

The viscosities of materials commonly encountered in everyday lives are summarized in Table 2. Liquid metal typically exhibits a viscosity similar to that of water. While, the viscosity of the current liquid slag is comparable to that of motor oil and honey. However, the half molten slag is expected to have a significantly higher viscosity, which would impede its flow.

Table 2. Viscosity of fluids (Pa.s)

Fluid at high temperature	Viscosity	Fluid at room temperature	Viscosity
$\text{SiO}_2\text{--CaO}$ slag	0.4–14.4	Ketchup [16]	60
$\text{SiO}_2\text{--FeO}$ slag	0.02–7.13	Honey [17]	10
		Moter Oil SAE [16]	0.07–0.32
		Diesel (kerosene) [16]	0.006
		Water [17]	0.001

3.7. Industrial application of the generated knowledge about slag formation

Slag formation and accumulation are not wanted in industrial furnaces for production of Si and FeSi. Large accumulation of slag will decrease the active reaction volume in the furnace and is believed to reduce the energy efficiency of the process. The mechanisms behind accumulation of slag in industrial furnaces is not yet understood. The findings from this study contribute with important knowledge about how to minimize slag accumulation in the furnaces and how to remove slag that has accumulated in the furnace. The knowledge that slags mainly are in equilibrium with the raw materials and that slag formation is independent of quartz source, shows the industry that it is not necessary to use special quartz source to avoid slag accumulation, but standard materials can be used. The differences between condensate and other silica sources show that investigations about reactions involving condensates must be targeted for future investigations about how to avoid slag accumulation.

The generated knowledge can also be used in optimisation and development of slag refining. The information about wetting angles are especially important for this.

4. Conclusion

This study investigates slag formation through reactions between limestone, iron source, and different silica sources (quartz, cristobalite, and SiO condensate) at milligram scale. Binary $\text{SiO}_2\text{--CaO}$ and $\text{SiO}_2\text{--FeO}$ slags reach equilibrium with solid SiO_2 between 1673–1973 K (1400–1700°C), with slag composition remaining consistent relative to SiO_2 particles. Slag forms more readily at 1573 K (1300°C) when

an iron source is present, compared to 1673 K (1400°C) with limestone alone. Minor elements accumulate on quartz grain boundaries before slag formation, while FeO and K_2O concentrations below 1wt% in slag outside the quartz. $\text{SiO}_2\text{--FeO--CaO}$ ternary slags are a mixture of solid and liquid between 1573–1873 K (1300–1600°C), resulting in slower dissolution compared to fully liquid slags. Neither the SiO_2 source nor phase (quartz or cristobalite) significantly affects slag formation. Si– SiO_2 –SiC condensate reacts with limestone to form $\text{SiO}_2\text{--CaO}$ slag with about 10wt% lower SiO_2 content than quartz or cristobalite reactions. Good wetting between $\text{SiO}_2\text{--FeO}$ or $\text{SiO}_2\text{--CaO}$ slags and quartz improves reactions, with stable wetting angles ranging from 0° to 47°. The study also shows that slag coalescence occurs before raw material softening, and the viscosity of the binary slags is comparable to everyday substances like motor oil or honey.

Acknowledgements

This work was financially supported by the Norwegian Ferroalloy Producers Research Association (FFF) and the Research Council of Norway through KSP project 326581 Recursive. They are both acknowledged.

Conflict of Interest

The authors declare that they have no known competing financial interests or personal relationships that could have appeared to influence the work reported in this paper.

Open access funding provided by {SINTEF}

Open Access This article is licensed under a Creative Commons Attribution 4.0 International License, which permits use, sharing, adaptation, distribution and reproduction in any medium or format, as long as you give appropriate credit to the original author(s) and the source, provide a link to the Creative Commons licence, and indicate if changes were made. The images or other third party material in this article are included in the article's Creative Commons licence, unless indicated otherwise in a credit line to the material. If material is not included in the article's Creative Commons licence and your intended use is not permitted by statutory regulation or exceeds the permitted use, you will need to obtain permission directly from the copyright holder. To view a copy of this licence, visit <https://creativecommons.org/licenses/by/4.0/>.

References

- [1] M. Gasik, *Handbook of Ferroalloys: Theory and Technology*, Elsevier, Oxford, 2013.
- [2] A.P. Shkirmontov, Energy parameters of ferrosilicon production with larger-than-normal values for the electrode gap and electrode spacing under factory conditions, *Metallurgist*, 53(2009), No. 9, p. 642.
- [3] M. Ksiazek, M. Tangstad, and E. Ringdalen, Five furnaces five different stories, [in] *Silicon for the Chemical and the Solar Industry XIII Proceeding, Trondheim*, 2016, p.33.
- [4] C. Sindland and M. Tangstad, Production rate of SiO gas from industrial quartz and silicon, *Metall. Mater. Trans. B*, 52(2021), No. 3, p. 1755.
- [5] S. Bao, M. Tangstad, K. Tang, and E. Ringdalen, Production of

- SiO gas in the Silicon Process, [in] *The Proceedings of 13th International Ferroalloys Congress Efficient Technologies in Ferroalloy Industry*, Almaty, 2013, p. 273.
- [6] B. Andrea and T. Merete, Condensation of SiO and CO in silicon production—A literature review, [in] *The First Global Conference on Extractive Metallurgy Proceeding*, Ottawa, 2018, p. 697.
- [7] A. Schei, J.K. Tuset, and H. Tveit, *Production of High Silicon Alloys*, Tapir Akademika Publishing, Trondheim, 1998.
- [8] M. Ksiazek and S. Bao, SiC forming reaction during the smelting of Si, [in] *Silicon for the chemical and the solar industry XVII Proceeding*, Trondheim, 2024, p.1, (2024), p. 1.
- [9] S. Jayakumari, *Formation and Characterization of β - and α -Silicon Carbide Produced During Silicon/Ferrosilicon Process* [Dissertation], Norwegian University of Science and Technology, Trondheim, 2020, p.53.
- [10] S. Jayakumari and E. Ringdalen, Effect of Varying SiO Contents on Si and FeSi, [in] *Silicon for the Chemical and the Solar Industry XVI Proceeding*, Trondheim, 2022, p.1.
- [11] M.B. Folstad, M. Ksiazek, and M. Tangstad, Slag in the tapping area in a Si furnace, [in] *Silicon for the Chemical and the Solar Industry XV Proceeding*, Trondheim, 2020, p.119.
- [12] M.B. Folstad, E. Ringdalen, H. Tveit, and M. Tangstad, Effect of different SiO₂ polymorphs on the reaction between SiO₂ and SiC in Si production, *Metall. Mater. Trans. B*, 52(2021), No. 2, p. 792.
- [13] E. Ringdalen and M. Tangstad, Softening and melting of SiO₂, an important parameter for reactions with quartz in Si production, [in] *Proceedings of the 10th International Conference on Molten Slags, Fluxes and Salts 2016*, Seattle, 2016) p. 43.
- [14] M. B. Folstad, *Slag and Its Effect on Si and FeSi Production* [Dissertation], Norwegian University of Science and Technology, Trondheim, 2023, p.67.
- [15] S. Bao, M. Tangstad, K. Tang, *et al.*, Investigation of two immiscible liquids wetting at elevated temperature: Interaction between liquid FeMn alloy and liquid slag, *Metall. Mater. Trans. B*, 52(2021), No. 5, p. 2847.
- [16] H. Dalaker, Viscosity of quartz-initial result from FactSage calculation [Report], SINTEF, Trondheim, 2020.
- [17] L. Zhu, X. He, X. Wu, J. Wu, and T. Hong, Recent development of abrasive machining processes enhanced with non-newtonian fluids, *Coatings*, 14(2024), No. 7, p.779.